

PAPER • OPEN ACCESS

Effect of CdS quantum dots size on Thermal and photovoltaic parameters of quantum dots sensitized solar cells

To cite this article: A. Khalid *et al* 2020 *IOP Conf. Ser.: Mater. Sci. Eng.* **762** 012007

View the [article online](#) for updates and enhancements.

Effect of CdS quantum dots size on Thermal and photovoltaic parameters of quantum dots sensitized solar cells

A. Khalid¹, K. Easawi¹, S. Abdallah¹, M.G.EL-Shaarawy², S. Negm¹, H. Talaat^{3*}

¹ Department of Mathematical and Physical Engineering, Faculty of Engineering (Shoubra), Banha University, Cairo, Egypt

² Physics Department, Faculty of Science, Benha University

³ Physics Department, Faculty of Science, Ain Shams University, Abbassia, Cairo, Egypt

* E-mail: : hassantalaat@hotmail.com

Abstract. The effect size of CdS Quantum Dots (QDs) on thermal and photovoltaic parameters is investigated. CdS QDs were adsorbed onto TiO₂ electrodes using successive ionic layer adsorption and reaction (SILAR) to act as sensitizers of quantum dots solar cells (QDSSCs). The CdS QDs sizes are estimated using optical absorption spectra and application of effective mass approximation model (EMA) as well as high resolution transmission microscopes (HRTEM). The ratio of TiO₂/CdS was confirmed by energy dispersive X-ray spectroscopy (EDX). Thermal parameters (thermal diffusivity α , thermal effusivity e and thermal conductivity k) are measured by using Photoacoustic (PA) Technique. The photovoltaic parameters (open circuit voltage V_{oc} , short circuit current density J_{sc} , fill factor FF and efficiency η) of the assembled CdS QDs sensitized solar cells (QDSSCs) were determined under a solar illumination of 100 mW/cm² (AM 1.5 conditions). Our results show that both the effective thermal conductivity k_{eff} and efficiency η of CdS QDs deposited on TiO₂ increase as the size of CdS QDs is increased.

Keywords: CdS QD; photoacoustic; SILAR; thermal properties

1. Introduction

The unique electronic and optical properties of semiconductor (QDs) have attracted significant attention to be used in QDSSC due to their large dipole moments and strong light absorption [1,2]. The dependence of their band gaps on their size makes them attractive candidates as sensitizers in photovoltaic solar cells because of the ability of tuning their band gap to the sunlight spectra [3, 4]. A regular QDSSC contains working electrode (TiO₂/QDs), redox electrolyte, and counter electrode [5, 6]. Successive ionic layer adsorption and reaction (SILAR) technique are among the better known methods used to synthesize QDs [7- 9]. SILAR is used in our study since it provides a good quality surface spread with the capability of tuning energy band gap through controlling QDs size with low costs technique [10-13]. Furthermore, it can simply adjust the thickness by controlling the number of cycles. Many studies were carried out using semiconductor QDs (especially CdS) [14] as sensitizers to fabricate QDSSCs. The photovoltaic performance of QDSSCs based on SILAR as QDs deposition technique is remarkably enhanced compared with those using the direct method. Measurement of thermal parameters such as thermal diffusivity (α), thermal effusivity (e) and thermal conductivity (k) for solar cell electrode are very essential to investigate the effect of rate of heat flow through the solar cell materials. More specifically K of the solar cell electrode is effect of operating temperature of solar cell. Photoacoustic technique (PA) is a photothermal detection technique; that is proved to be a powerful tool to study the optical and thermal properties of such Materials without particular sample treatment in a nondestructive manner [15-17]. In PA technique only the absorbed light energy contributes in the form of heat, while the scattered and reflected parts of light don't contribute



to the PT signals. Accordingly, PT spectroscopy more accurately measures optical absorption and thermal properties in highly scattering QDSSCs. Modulating of incident photon intensity causes temperature pulsations and the resulting temperature variation at the surface causes pressure variation in the PA cell [18]. Such pressure fluctuations can be detected by a sensitive microphone and constitute PA signal.

In this work CdS QDs were synthesized onto TiO₂ NPs by SILAR technique through increasing number of cycles under ambient conditions. The particles sizes were determined using (EMA) as well as HRTEM. The ratio of TiO₂/CdS was confirmed by (EDX). The size dependence of α , ϵ and k for CdS QDSSs working electrode has been measured using PA technique. Also, the photovoltaic characteristic of the QDSSs (short current density J_{sc} , open circuit voltage V_{oc} , fills factor FF and efficiency for energy conversion η) are measured as a function of the varying size of CdS QDs.

2. Experimental

2.1. Deposition of the CdS QDs onto TiO₂ NPs photoelectrode

A colloidal paste of TiO₂ NPs was prepared according to our previous work [19]. The TiO₂ paste was deposited on a conducting glass substrate of Florien Tin Oxide SnO₂:F (FTO) with sheet resistance of 7 Ω /sq and > 80% transmittance in the visible region, using a simple doctor blade technique. This was followed by annealing at 450 °C for 30 min and the final thickness was 8 μ m after the solvent evaporation.

The TiO₂ photoanodes were sensitized with CdS QDs using SILAR method [20]. Where the photoanode is immersed for one min in 0.1 M (Cd(NO₃)₂.H₂O) in methanol as a cation source (Cd⁺²) to be adsorbed on the TiO₂ electrode. The TiO₂ electrode was then rinsed with methanol to remove the excess Cd⁺² cations. Then the photoanode is immersed in 0.1 M Na₂S methanolic solution as the anion source (S⁻²) for one min in order to react with Cd⁺² cations followed by methanol rinsing. This procedure constitutes as one SILAR cycle. Five samples obtained by increasing number of layer thickness of cycles were labeled a, b, c, d and e for 2, 4, 6, 8 and 10 cycles, respectively. The counter electrodes were prepared by coating another FTO substrate of resistance of 7 Ω /sq with platinum (Pt).

2.2. Assembly of QDSSCs

QDSSCs were built as shown in Figure 1 by assembling the TiO₂ photoanodes sensitized with CdS QDs, aqueous polysulfide electrolyte and the counter electrodes. Parafilm was used as spacer between the two electrodes and also as a sealing to prevent the evaporation of the electrolyte. The space between the two electrodes was filled by polysulfide electrolyte which was prepared by dissolving 1.1M Na₂S, 1.2 M S, and 0.12 M KCl in deionized water. The counter electrodes were prepared by coating another FTO substrate of resistance of 7 Ω /sq with platinum (Pt).

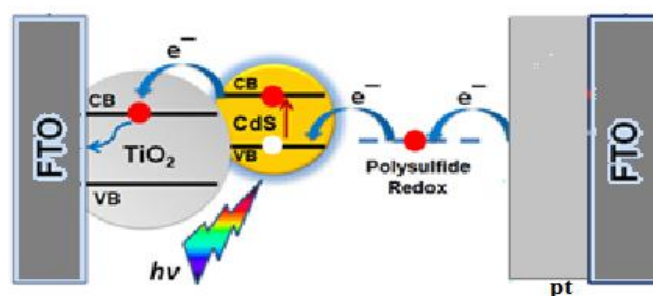


Figure1. Schematic representation of the assembled QDSSCs

2.3. Measurements

The optical absorption spectra of the working electrode (TiO₂/CdS) were measured using a UV–Visible spectrophotometer (JASCO V-670). The particle size of sample was measured using transmission electron microscope (TEM) (JEOL JEM-2100). The PA Thermal measurements were carried out using PA cell with a gas microphone detection technique and argon ion laser 6 W (514 nm) . The PA signal generated from the sample was amplified by a low noise preamplifier and further processed using a lock-in amplifier (Stanford Research System, Model SR830 DSP). A personal computer was interfaced to the system for automatic data acquisition and analysis

The current density voltage (J–V) characteristics are recorded with a Keithley SMU 2400 voltage source ammeter. The CdS QDSSCs were subjected to the irradiation of a solar simulator (San-Ei Electric XES-40S1) operating at 100 mW/cm² (AM 1.5G). The incident solar intensity illumination was adjusted to 1 sun condition using a Leybold certified silicon reference solar cell (Model: Bunkoukeiki BS-500BK). A J-V.

Characteristic curves of CdS QDSSCs with five particle sizes were obtained and all experiments were carried out under ambient conditions. The photoelectric conversion efficiency η was determined according to:

$$\eta = \frac{P_{max}}{P_{in}} \% = \frac{V_m I_m}{P_{in}} \% \quad (1)$$

Where V_m and I_m are the maximum voltage and current respectively.

The fill factor FF is given by :

$$FF = \frac{V_m I_m}{V_{oc} I_{sc}} \% \quad (2)$$

3. Results and Discussion

3.1. Optical measurements of CdS QD

TiO₂/CdS layer in ethanol was scratched from FTO coated substrate without disturbing FTO layer and placed on Cu-coated carbon grid for TEM measurement. Figure 2 shows the TEM image of TiO₂/CdS for sample (e) , the average particle size for CdS QD were estimated to be approximately 5.4 nm and average particle size for TiO₂ is 22 nm.

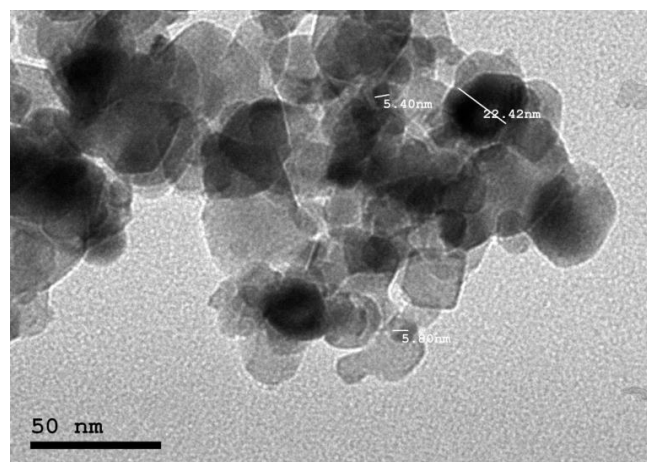


Figure 2. TEM micrographs of TiO₂/ CdS for sample (e)

Figure 3 show UV-visible absorption spectra for FTO/TiO₂ and FTO/TiO₂ / CdS photoanode with increasing number of SILAR cycles. It can be seen that the TiO₂ layer shows an absorbance edge at 400 nm corresponding to 3.1 eV band gap for TiO₂ nanoparticles. Also, there is a red shift of absorbance edge with increasing number of cycle. Samples a, b, c, d and e has peak absorption are 401 nm, 414 nm, 431 nm, 451nm and 465 nm for, respectively.

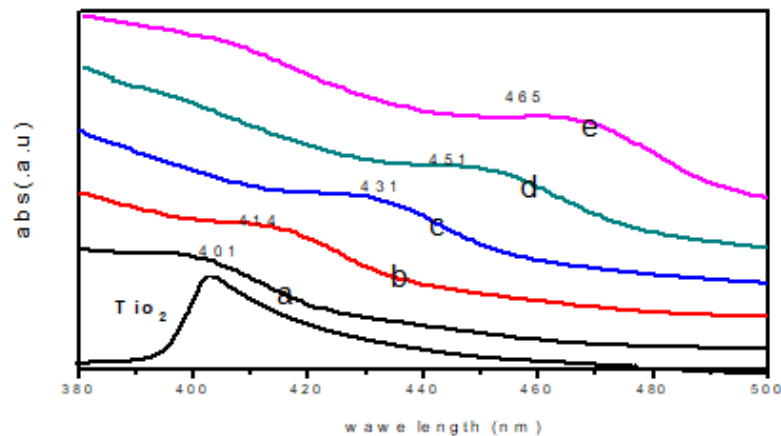


Figure 3. UV –Visible absorption spectra for TiO₂ and five TiO₂/CdS QDs samples with different number of cycles by SILAR method

The corresponding particle sizes of CdS QD are calculated using the effective mass approximation (EMA) [21].

$$E_{gn}(R) = E_{gb} + \frac{h^2}{8m^*R^2} - \frac{1.8e^2}{4\pi\epsilon\epsilon_0R} \quad (3)$$

where E_{gb} (2.4 eV) is the bulk CdS band gap, E_{gn} is the nanoparticle band gap, R is the radius of the CdS quantum dots, m^* (7.62×10^{-32} kg) is the reduced electron-hole mass, and ϵ (7.1) is the dielectric constant for CdS [22]. The obtained values of CdS particle sizes are 3.21 nm, 3.4 nm, 3.7 nm, 4.01 nm and 4.4 nm for samples a, b, c, d and e, respectively in close agreement with that obtained by TEM measurements. EDX determined by (JEOL JED-2300). Figure 4 shows the EDX spectra of TiO₂/CdS QDs sensitized working electrode where Cd, S, Ti and O atoms are indicated. The adsorption of CdS QDs onto the TiO₂ working electrode was confirmed by EDX.

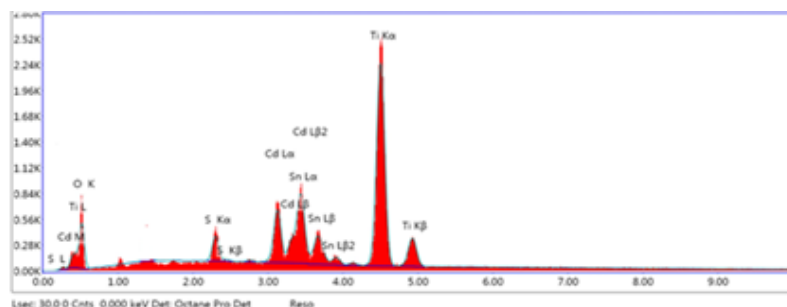


Figure 4. EDX of TiO₂/ CdS QD working electrode for sample e

3.2. Thermal measurements:-

The PA technique was employed to investigate the effective thermal parameter of (FTO/TiO₂/CdS QDs) photoanode that are important for solar energy conversion. Assuming that this photoanode as effectively FTO/TiO₂ and CdS QDs. The PA signal amplitude was recorded at various chopping frequencies (f) for each of the size photoanodes. The change of ln PA amplitude is plotted versus ln f for FTO/TiO₂ substrate is seen in Figure 5. A distinct change in the slope is clearly observed at a particular frequency f_c where the sample changes from being thermally thick to thermally thin where the crossover takes place [23].

The thermal diffusivity (α) of working electrode is then calculated using the relation [24].

$$\alpha_{\text{eff}} = f_c L^2 \quad \text{in } \text{m}^2/\text{s} \quad (4)$$

where L is the working electrode thickness. The obtained value D is about $3.2 \times 10^{-5} \text{ m}^2/\text{s}$. The plots of ln PA amplitude versus the ln f for photoanode (FTO/TiO₂/CdS QDs) of different CdS QDs sizes are shown in Figure 6(a), 6.b, 6.c, 6.d and 6.e for sample a, b, c, d and e, respectively. The calculated values of α_{eff} are displayed in Table 1. The results showed that, there is an increase of α_{eff} with increasing CdS QDs sizes which was about 216 % from its original value for the highest CdS QDs size.

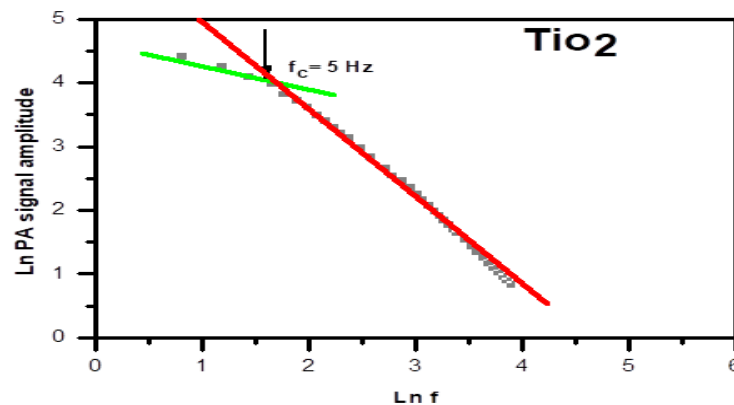


Figure 5. Variation of ln PA signal amplitude versus ln f for FTO/TiO₂.

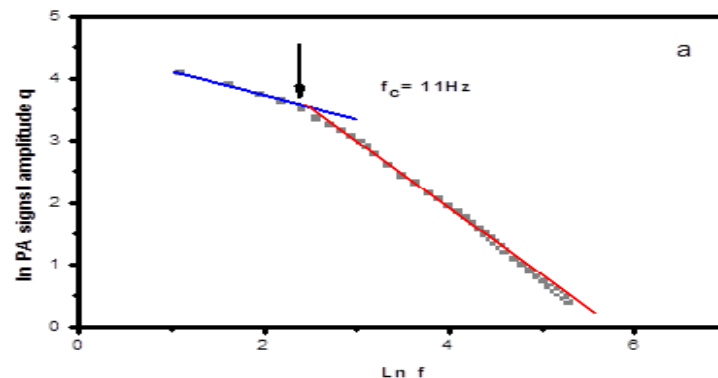


Figure 6.a Variation of ln PA signal amplitude versus ln f for sample a of FTO/TiO₂/CdS QDs.

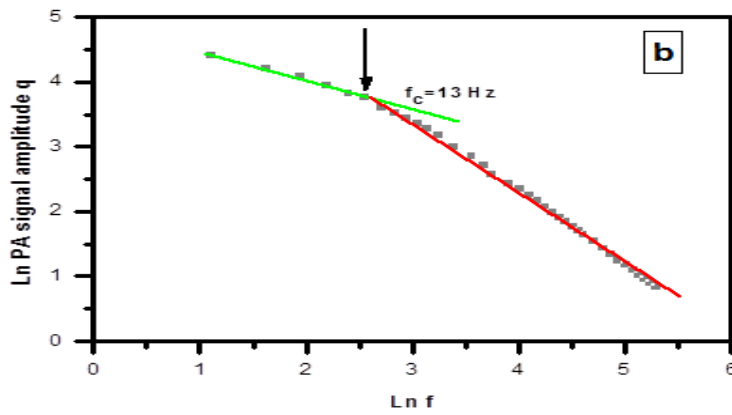


Figure 6.b Variation of ln PA signal amplitude versus ln f for sample b of FTO/TiO₂/CdS QDs.

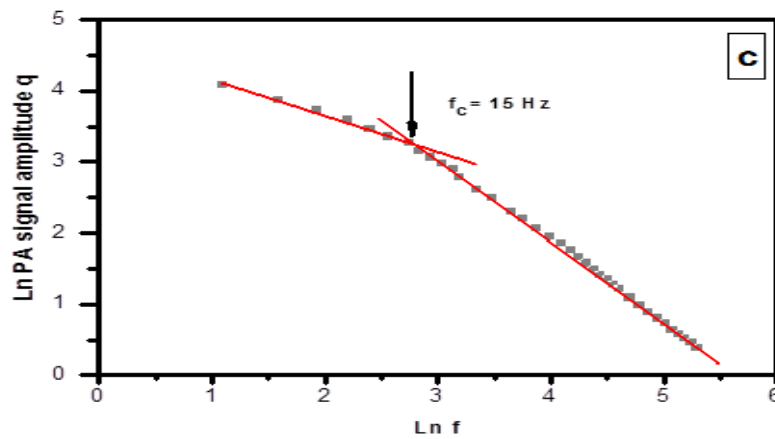


Figure 6.c Variation of ln PA signal amplitude versus ln f for sample c of FTO/TiO₂/CdS QDs.

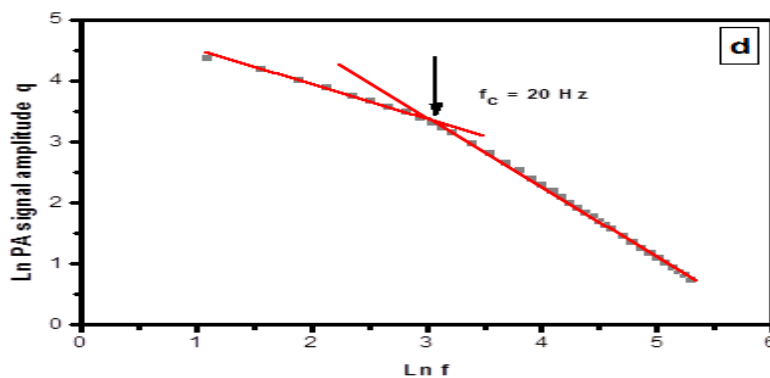


Figure 6.d Variation of ln PA signal amplitude versus ln f for sample e of FTO/TiO₂/CdS QDs.

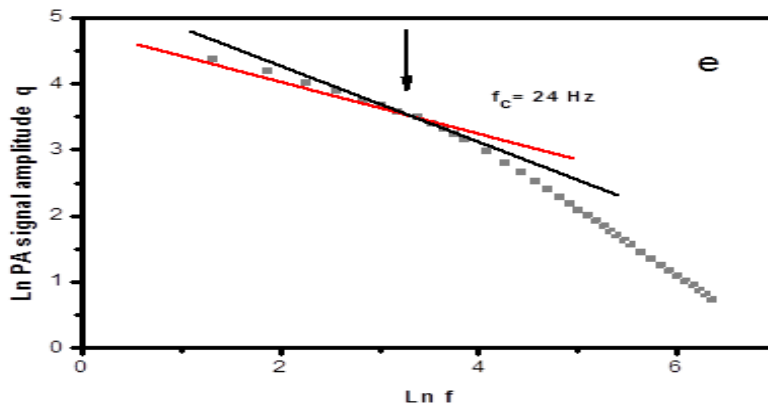


Figure 6.e Variation of Ln PA signal amplitude verses Ln f for sample e of FTO/TiO₂/CdS QDs.

The plots of ln (PA) against 1/ f for the same photoanode are seen in Figure 7 .The effective thermal effusivity e_{eff} were also estimated for our samples which are, thermally thick , hence the signal amplitude of PA is given by [25].

$$q = \frac{A}{e} \frac{1}{f} \tag{5}$$

where
$$A = \frac{I_0 \gamma P_0 \alpha_g^{1/2}}{4 \pi l_g T_0}$$

I_0 is the incident radiation intensity; T_0 and P_0 are the ambient pressure and temperature respectively, γ is gas specific heats ratio, α_g is the gas thermal diffusivity and l_g is the length of the gas column of the PA cell. Using the Si as a standard material of known effusivity ($=16061 \text{ W.s}^{1/2}.\text{m}^{-2}.\text{K}^{-1}$)[18], the constant A was determined and applied in equation (5) to calculate e_{eff} for the photoanode with different CdS QDs. Size. The values resulting of e_{eff} are given in Table 1. The results show that the values of e_{eff} of photoanode increased from $4785 \text{ W.s}^{1/2}.\text{m}^{-2}.\text{K}^{-1}$ to $6071 \text{ W.s}^{1/2}.\text{m}^{-2}.\text{K}^{-1}$ as the CdS QDs size increase from 3.21 nm to 4.4nm. The measured values of α and e ($3.2 \times 10^{-5} \text{ m}^2/\text{s}$ and $1502 \text{ W.s}^{1/2}.\text{m}^{-2}.\text{K}^{-1}$) for FTO/TiO₂ substrate are used to calculate its thermal conductivity k ($=e\sqrt{\alpha} = 8.5 \text{ W/m. K}$).The calculated values of our photoanode effective thermal conductivity (k_{eff}) of CdS QDs sizes are also given in Table 1. There is an increase of k_{eff} with increasing the CdS QDs sizes, and is about 186 % for largest size 4.4 nm

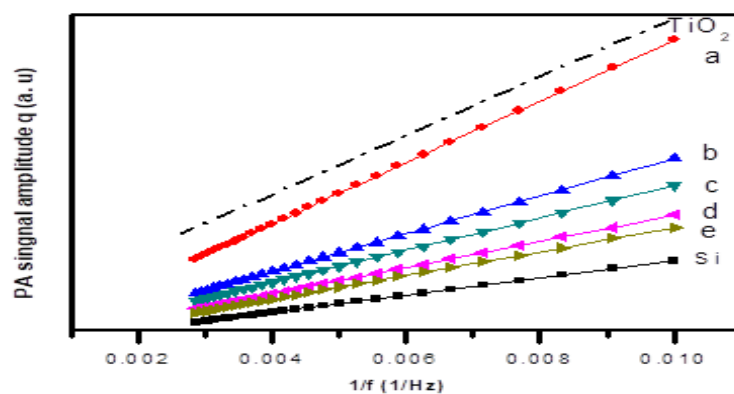


Figure 7. PA signal amplitude versus 1/f for sample a to sample e

Table 1. The calculated values of effective thermal diffusivity α_{eff} , effective thermal effusivity e_{eff} and effective thermal conductivity k_{eff} for TiO₂/ CdS QDs samples of different particle sizes.

sample	CdS particles sizes nm	(α_{eff}) ($10^{-5} \text{ m}^2/\text{s}$)	(e_{eff}) ($\text{Ws}^{1/2}\text{m}^{-2}\text{K}^{-1}$) ± 7	(k_{eff}) (W/m. K)
A	3.21	7.1 \pm 0.05	4785	40.32 \pm 0.14
B	3.4	8.4 \pm 0.05	4975	45.60 \pm 0.14
C	3.7	9.6 \pm 0.05	5383	52.75 \pm 0.13
D	4.01	13.1 \pm 0.05	5908	67.63 \pm 0.11
E	4.4	15.4 \pm 0.05	6071	75.35 \pm 0.11
FTO/TiO ₂	-	3.2 \pm 0.05	1502	8.5 \pm 0.12

It is easily observed that, as the number cycles increase the values of α_{eff} , e_{eff} and k_{eff} are increase. In an earlier work [15, 25], the thermophysical parameters of CdSe and CdTe QDs determined using PA technique, showed that the values of α , e and k decrease as QDs size increases. In the present case of SILAR technique, the produced CdS QDs are produced impregnated in the TiO₂ pores; decreasing the space, hence increase the thermal conductivity of the materials [26]. This results is in different to the regular chemical sensitizes technique.

3.3. Photovoltaic performance of CdS QDSSCs

The J-V characteristics curves of CdS QDSSCs are shown in Figure 8. The photovoltaic parameters V_{oc} , J_{sc} , FF and η for CdS QDSSCs are given in Table 2. It is clearly seen that as CdS QDs size increases, the values of J_{sc} and η increase. The maximum values of J_{sc} and η are 2.24 mA/cm² and 0.48% for sample e 4.4 nm (10 cycles) sample e of CdS QD. S.Abdallah et. al [27.28] has made measurement on CdS QD sensitized TiO₂ using the direct adsorption (DA) technique. They reported that, an increase of J_{sc} (from 0.31 mA/cm² to 0.67 mA/cm²) and η (from 0.05% to 0.18%) as the particle size increase 3.14 to 3.84 nm. The present results shows an increase of J_{sc} from 1.18 mA/cm² to 2.24 mA/cm² and η from 0.15% to 0.48% with increasing particle size from 3.21 nm to 4.4 nm of CdS QDs compatible with previous work. They attributed the increase in J_{sc} with increase particle size in and red shift of the absorption edges harvesting more visible photons in the solar spectrum and thus causes relativity high absorption of the incident photon from solar spectrum. The Improvement of the J_{sc} and η in the case of SILAR technique is being better method than DA give high-quality surface spread, lower aggregation and higher photocurrents, [29].

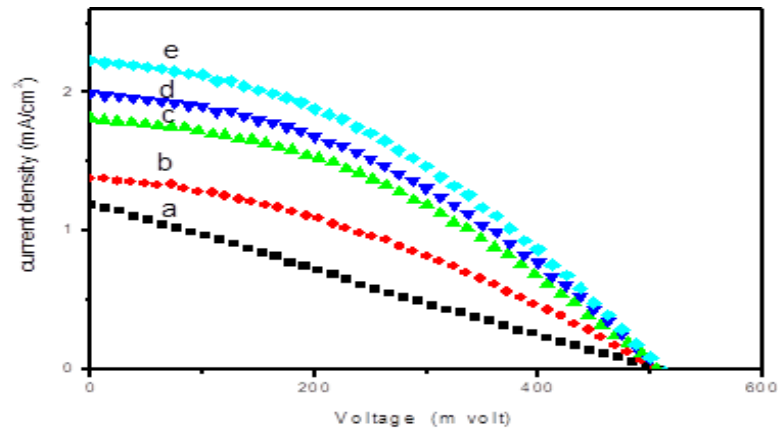


Figure 8. J-V characteristic curve of QDSSCs of CdS QDs with different different cycle

Table 2. J -V characteristics parameters of a CdS QDSSCs for different QDs sizes, under 1 sun illumination.

Sample	CdS particles sizes nm	V_{oc} (m Volt) ± 0.01	J_{sc} (mA/cm ²)	FF	η (%) ± 0.01
a	3.21	508	1.18 ± 0.01	0.24	0.15
b	3.4	505	1.38 ± 0.02	0.35	0.24
c	3.7	504	1.82 ± 0.01	0.39	0.37
d	4.01	509	2.01 ± 0.01	0.38	0.42
e	4.4	510	2.24 ± 0.01	0.40	0.48

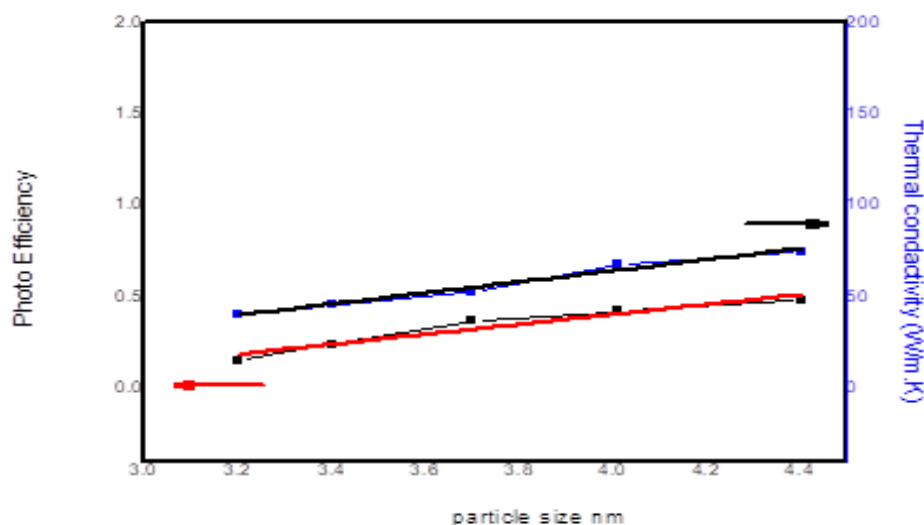


Figure 9. The relation between thermal conductivity k and photo efficiency η with QDs particle size

The variation of η and k_{eff} as function CdS QD particles size are shown in Figure 9. There is an increase in η and k_{eff} as the size of CdS QDs increase. The increase of thermal conductivity would lead to the decrease the dissipation of local heat in the solar cell and less recombination.

4. Conclusion

CdS QDs of different sizes were adsorbed onto TiO_2 nanoparticle electrode using SILAR method of varying to obtain varying layers of CdS QDs as sensitizer for QDSSCs. EDX measurements ensure the success of adsorption of CdS QDs onto the TiO_2 electrode. The UV spectra show a shifted to lower energy region from 3.07 eV to 2.70 eV as the number of cycles increase from 2 to 10 cycles. The average particle sizes were estimated using EMA to be 3.21 nm to 4.4 nm which was confirmed by TEM. The thermophysical parameter e_{eff} , α_{eff} and k_{eff} of FTO/ TiO_2 /CdS photoanode of different cycles, are determined by PA technique, show an increase with increasing cycle. The increase of k_{eff} is explained by, the increase of number of cycle results a reduction of air and oxygen molecules impregnated inside the TiO_2 microspores. The increase of values of J_{sc} and η of CdS QDs solar cells with the number of cycles i is mostly attributed to better matching with solar spectrum. Furthermore, the increase of thermal conductivity leads to the decrease the dissipation of local heat and hence less recombination.

5. Acknowledgements:

The authors would like to express their sincere gratitude to Ain Shams University and the Physics Department at Ain Shams University for their financial and technical support in performing and finishing this work.

References

- [1] Okate, K. , Kunita,S. , Jagtap, C. V. , Baviskar,P. K. , Jadkar,S. R., Pathan, H. M., & Mohite, K. C. (2018).*Optik-International J. for Light and Electron Optics*, 157 ,628-634.
- [2] Tubtimtae,A. , Lee,M. W., & G. Wang,J. (2011). *J. Power Sources* ,196 ,6603–6608.
- [3] Salant,A. , Shalom,M., . Hod, I, Faust,A. , Zaban A. , & Banin, , U. (2010). *ACS Nano*, 4 ,5962–5968.
- [4] Kongkanand,A., Tvrdy,K., Takechi,K., Kuno,M., & Kamat,P.V. (2008). *J. Am. Chem. Soc.*, 130, 4007–4015.

- [5] Badawi,A., Obdallah,W., AL-Baradi,A.M. & AL-hosiny, N. (2019). *Mater. Sci. Semicond. Process.*,95,1-12.
- [6] Badawi,A., Al-Hosiny,N., Abdallah,S., & Talaat, H., ,(2013). *Mater. Sci.-Poland* ,31, 6–13.
- [7] Badawi,A., Al-Hosiny,N., & Abdallah,S. (2015). *Superlat. and Micro.*, 81, 88–96.
- [8] Zhang,Y, Zhu,J., Yu,X., Wei, J., Hu,L. & Dai,S. (2012). *Sol. Energy*, 86,964–971.
- [9] M.P. Valkonen, S. Lindroos and M. Leskelä, *Appl. Surf. Sci.* 134 (1998). 283–291.
- [10] Laukaitis,G. , Lindroos,S. , Tamulevičius,S. , Leskelä,M. , & M. Račkaitis, (2000).*Appl. Surf. Sci.* ,161,396–405.
- [11] Bailey ,R.E., & Nie, S., (2003) *J. Am. Chem. Soc.*, 125, 7100–7106.
- [12] Badawi,A., *J Mater Sci: Mater Electron*, DOI 10.1007/s10854-016-4781-1.
- [13] Badawi,A. ,(2016) . *Superlatt. and Micro.*, 90 124-131.
- [14] Badawi,A., Al-Hosiny, N., Abdallah, S., Merazga,A., & Talaat, H. ,(2014). *Mater. Sci. Semicond. Process.*, 26, 162.
- [15] Al-Hosiny ,N., Badawi ,A., A.Moussa,M.A., El-Agmy, R., & Abdallah,S. (2012).*Int. J. Nanopart* 5,258–266.
- [16] Abdallah ,S., El-Brolossy,T.A., Negm,S. , & Talaat,H. (2008).*Eur.Phys.J.Spec. Top.*,153,199–202.
- [17] A.Rosencwaig,A.Gersho, (1976).*J.Appl.Phys.*47,65–69.
- [18] El-Qahtani ,Z., Badawi , A., Easawi ,K., Al-Hosiny, N. , & Abdallah,S. (2014),*Mater. Sci. Semicond. Process.* 20,68–73.
- [19] Syrokostas,G., Giannouli,M., &Yianoulis,P. (2009), *Renewable Energy* ,34,1759–1764.
- [20] Lee,Y., & Lo,L. ,(2009) *Adv. Funct. Mater.* ,19,604–609.
- [21] Talaat,H.,Abdallah,T.,Mohamed,M.B.,Negm,S., &El-Sayed,M.A.,(2009),*Chem.Phy.Lett.*,473,288-292.
- [22] Khalid,A., Easawi,K., El-Shaarawy,M. G., Negm,S., & Talaat, H. (2010). *Egypt. J. Solids*, 33 ,211-218.
- [23] El-Brolossy,T.A., Abdallah,S., Abdallah, T., Mohamed,M.B. , Negm ,S., & Talaat,H., (2008). *Eur. Phys. J. Special Topics*, 153, 365.
- [24] Raji, P. , Sanjeeviraja,C. , & Ramachandran, K.,(2004). *Cryst. Res. Technol* ,39,617–622.
- [25] Badawi,A., Al-Hosiny,N., Abdallah,S., Negm,S., & Talaat,H. ,(2012) *J. of mater. Scien. and engineer.*,1,1-6.
- [26] El-Brolossy, T.A., ,(2012).*Indian J. Phys.* ,86,39-44.
- [27] Abdallah, S. , Al-Hosiny N., & Badawi,A., (2012)*MSTI-Nanoteck*,1,55-60.
- [28] Abdallah, S. , Al-Hosiny N., & Badawi,A., (2012) *J. of Nanomaterial*,1,1-6.
- [29] Li ,W., & Zhong X., (2015) *J. phys. Chem. Lett.* , 6,796-806.